Colloids and Surfaces A: Physicochemical and Engineering Aspects 648 (2022) 129231

Contents lists available at ScienceDirect

Colloids and Surfaces A: Physicochemical and Engineering Aspects

journal homepage: www.elsevier.com/locate/colsurfa

Opposite effect of cyclic and chain-like hydrocarbons on the trend of self-assembly transition in catanionic surfactant systems

Shasha Jiang [a,b], Xiaoyu Li [a], Shuitao Gao [a], Cheng Ma [a], Tongyue Wu [a], Zhijie Liu [a], Ting Gu [a], Jinwan Qi [a], Yun Yan [a], Xinmin Song [c,*], Jianbin Huang [a,*]

[a] College of Chemistry and Molecular Engineering, Peking University, Beijing 100871, China
[b] School of Earth & Space Science, Peking University, Beijing 100871, China
[c] State Key Laboratory of Enhanced Oil Recovery, Research Institute of Petroleum Exploration and Development, Beijing 100083, China

GRAPHICAL ABSTRACT

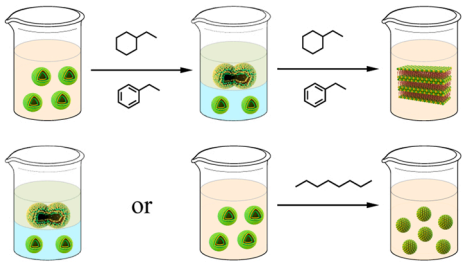

ARTICLE INFO

Keywords:
Catanionic surfactant system
Structure of hydrocarbon
Soluble location
Aggregate behavior

ABSTRACT

Hydrocarbons are well-known insoluble oils which are rarely considered as stimuli to trigger molecular self-assembly transition. We report in this work that hydrocarbons are a class of distinct stimuli for the self-assembly transition in the catanionic surfactant systems. Particularly, the cyclic hydrocarbons and chain-like ones has exactly opposite impact. By solubilizing in the palisade region of surfactant bilayers, the cyclic hydrocarbons would increase the volume of the hydrophobic part of the surfactant, thus increasing the packing parameter and leading to structures with smaller curvature. On the contrary, the chain-like hydrocarbons will be insolubilized in the interior of the hydrophobic domains formed by surfactant, which therefore swells the surfactant bilayers and increases the curvature of the outer layer. As a result, the self-assembly would change into structures with larger curvature. For this reason, addition of cyclic alkanes, such as ethylcyclohexane and ethylbenzene, leads to the transition from vesicles to lamellae, whereas addition of chain-like ones, such as octane, results in the transition from vesicles or lamellae to nanoemulsions. It is noticed that the saturation state of the hydrocarbons is not relevant to the self-assembly transition, and whether the alkanes are cyclic or chain-like is the determinative factor that decides which direction the self-assembly would transform to. We expect the current study is very promising in guiding enrichment and separation of organic matters.

* Corresponding authors.
E-mail addresses: Sxm@petrochina.com.cn (X. Song), jbhuang@pku.edu.cn (J. Huang).

https://doi.org/10.1016/j.colsurfa.2022.129231
Received 2 April 2022; Received in revised form 6 May 2022; Accepted 11 May 2022
Available online 14 May 2022

1. Introduction

Surfactants have drawn much attention from researchers and have been widely utilized in many fields, such as industrial manufacturing [1–4], agricultural production [5–10] and fundamental research [11, 12] owing to their ability to form a rich variety of self-assembled structures, such as micelles [13], vesicles [14–16] and lamellae [17]. Transitions between these self-assembled structures are often accompanied with useful applications [18,19]. For example, vesicular transitions from isolated to densely packed states can cause phase separation to give aqueous surfactant two-phase (ASTP), which is very promising in extracting various biomolecules and separation of conductive carbon nanotubes from the semi-conductive ones [20,21]. Therefore, tailoring the morphology of surfactant self-assembly in a controllable manner is highly desired.

Catanionic surfactant systems (mixed cationic/anionic surfactant systems) are well-known for their abundant self-assembled structures that are sensitive to mixing ratios [12,22,23]. Self-assembly transition may occur if an external stimulus triggers the change of the mixing ratio between the two oppositely charged surfactants [24]. This is particularly true at molar ratios close to charge balancing [25]. Compared to numerous studies about the effect of light [25,26], temperature [27,28], salt [29–31], and pH [21,32,33] on the self-assembly transition in cat-anionic surfactant systems, little attention has been paid on the impact of hydrocarbons [34], since they are usually considered as insoluble oils, rather than external stimuli.

In fact, hydrocarbons indeed play important roles in the self-assembly transformation in catanionic surfactant systems. For instance, Mao et al., [35,36] found that catanionic vesicles could turn into rod-like micelles and eventually to spherical micelles on addition of octane, but drastic enlargement of vesicles and the formation of lamellar structures were observed if toluene was added. The opposite trend of self-assembly transition indicated that the polarity or structure of hydrocarbons might be very crucial in tailoring the self-assembly morphologies in catanionic surfactant systems. Nevertheless, so far, the study in this regard is far less than enough.

To investigate the decisive factor of apolar hydrocarbon in regulating the self-assembling behavior of catanionic surfactants, herein we compared the effect of two categories of hydrocarbons, namely, chain-like and cyclic ones, on the self-assembly transition in the catanionic surfactant systems of dodecyl dimethyl benzyl ammonium chloride (BDDAC)/ sodium octyl sulfonate ($SOSO_3$) at molar ratios close to charge-balance. To this goal, we either started from the ASTP, or from the homogenous system at the edge of ASTP. We found that hydrocarbons with cyclic structures, regardless their polarity, tend to decrease the curvature of the self-assembled structures, whereas the chain-like alkanes would increase the curvature. The polarity, or the saturation status of the hydrocarbons was not relevant to the self-assembly transition. This fact indicated that cyclic hydrocarbons would be solubilized in palisade layer of the surfactant bilayers which would increase the volume of the hydrophobic chains and sufficiently shield the net charges between the ionic surfactant heads, leading to the growth of the self-assembled structures. On the contrary, the chain-like alkanes would be solubilized in the interior of the hydrophobic region, which swelled the interior, and resulted in larger curvature in the outer layer. As a result, the size of the self-assembled structures tended to be diminished. For this reason, addition of cyclic hydrocarbons to a homogeneous catanionic surfactant vesicular system would cause ASTP, whereas addition of chain-like alkanes to the same system would result in homogeneous phases composed of nanoemulsions. We expect the current findings would have potential applications in the field of separation and nano encapsulation.

2. Experimental section

2.1. Materials

Sodium octyl sulfonate ($SOSO_3$, 99%) was purchased from Macklin. Benzyldimethyldodecylammonium chloride (BDDAC, 99%) was purchased from TCI. Octane (AR) and ethylbenzene (AR) were obtained from Sinopharm Chemical Reagent Co., Ltd. Ethylcyclohexane (99%) was purchased from Aladdin. Pyrene and diphenylhexatriene (DPH) are A. R. grade from Sigma. All reagents were used as received. Milli-Q water of 18 MΩ is used to prepare aqueous solutions.

2.2. Sample preparation

Desired concentrations of surfactant stock solutions were prepared in volumetric flask. Samples were then obtained by directly mixing the solutions of anionic and cationic surfactants at a desired mixing ratio and concentration. BDDAC and $SOSO_3$ in the wide C_T (total concentration) of 20–100 mM was used in this study. After sealing, surfactant solutions together with organic additives were vortically mixed and then equilibrated in a temperature incubator at 25 °C for 3 days prior to the observation and other experiments.

2.3. Negative-staining trans mission electron microscopy (NS-TEM)

NS-TEM measurements were taken by Tecnai T20 and functioned at an accelerating voltage of 200 kV. A drop of the sample (~10 μL) was placed onto a carbon-coated copper grid (300 mesh) and was stained with 3% uranyl acetate for 3 min. Excess sample and staining agent were removed by filter paper. All samples were allowed to dry in ambient air at room temperature prior to the observations.

2.4. Freeze-fracture transmission electron microscopy (FF-TEM)

Freeze fracture and replication technique were performed to evaluate the microstructures of surfactant solutions. First, a specimen holder with a small drop of the as-prepared solution was cooled by liquid nitrogen. Then, a high-vacuum freeze-fracture apparatus (Balzers BAF 400D) was employed to fracture and replicate the specimen. Finally, the replicas composed of a thin layer of carbon were shifted onto copper grids and were ready for the TEM measurement on Tecnai T20 (200 kV).

2.5. Rheology

The rheological properties of all the samples with a volume of 10 mL were evaluated with a Thermo Hake RS300 rheometer at 25 °C.

2.6. Ultraviolet-visible spectrophotometer

UV–vis absorbance measurements were performed using a UV-1800 SHIMADZU spectrophotometer (Hitachi. Ltd., Tokyo, Japan), and 1 cm quartz cuvettes were used. All spectral measurements were recorded at 25 °C.

2.7. Dynamic light scattering (DLS)

DLS data were recorded on a BI-200 SM instrument. The samples were filtered by 800 nm filters prior to the observations. All measurements were performed using deionized water at 25 °C.

2.8. Fluorescence spectrometry

Fluorescence spectra were collected on a Hitachi F7000 spectrometer using a constant temperature bath to control the temperature to be 25 °C.

2.9. Polarized optical microscopy (POM)

The representative photographs of samples with lamellar structures under a polarization microscope were carried out by an Axioscope 5 POM.

3. Results and discussion

3.1. Phase behaviors and microstructures of BDDAC/$SOSO_3$ mixed system

The phase diagram of BDDAC/$SOSO_3$ catanionic surfactant systems at 25 °C is given in Fig. 1**a**. Precipitates occur in a broad range of x_{BDDAC} as the total surfactant concentration is lower than 80 mM, whereas the precipitation region narrows at much higher concentrations. ASTP occurs in both the BDDAC-rich and $SOSO_3$-rich sides, which is labeled as C-ASTP and A-ASTP, respectively. The representative photos of the phase status for samples at C_T of 100 mM is given in Fig. 1**b.** At the BDDAC-rich sides (x_{BDDAC}≥0.50), precipitates, which float at the surface of the system, occurs at x_{BDDAC}= 0.50. The initial transparent solution gradually turns to opalescent, separates to ASTP, becomes homogeneous birefringent, as the system composition is gradually approaching to x_{BDDAC}= 0.50 from both sides.

The microstructures in these phases are further studied with TEM and DLS. Spherical particles with the diameter of 5 nm are present in the transparent homogeneous solutions with x_{BDDAC}≥ 0.70 (Fig. S1a**)**. In the range of 0.70 > x_{BDDAC}≥ 0.67 where the system is opalescent but still homogeneous, and vesicles are observed (Fig. S1b**)**. In the ASTP systems with x_{BDDAC} between 0.67 and 0.66, large vesicles with diameter of 2 μm and small ones about 100 nm are found in the upper and lower phases, respectively (Fig. S1c**)**. The microstructures in the homogeneous birefringent system (0.66 > x_{BDDAC}≥0.58) with Maltese crosses textures under POM are the lamellar structures (Fig. S2a, Fig. S1d**)**. The variation of the self-assembled structures in the BDDAC-rich sides as the surfactant composition approaching to 1:1 is summarized in Fig. 1**c**. In the $SOSO_3$-rich sides, similar self-assembled structures are observed with increasing x_{BDDAC} (Fig. S1e**-f)** and lamellae are collaboratively confirmed by POM (Fig. S2b**)** and FF-TEM (Fig. S1e**)**.

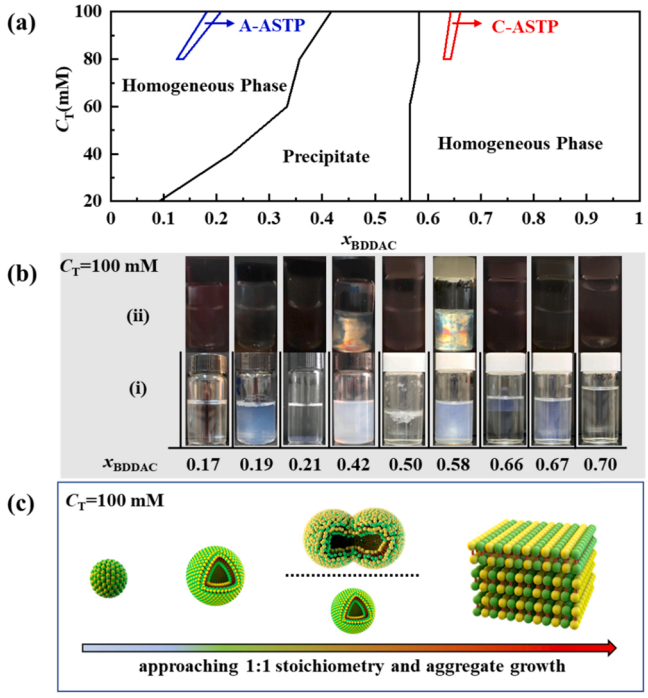

Fig. 1. (a) Phase diagram for BDDAC/$SOSO_3$ mixed systems at 25 °C. (b) Photographs of BDDAC/$SOSO_3$ mixed systems at different mixing ratios (C_T =100 mM, 25 °C): (i) under visible light, (ii) under the polarizer. (c) Schematic illustration of the aggregates in BDDAC-rich BDDAC/$SOSO_3$ mixed systems (C_T =100 mM, 25 °C).

3.2. Phase behavior and organized assemblies transition in mixed BDDAC/$SOSO_3$ systems with organic additives

3.2.1. Homogeneous phase for addition of organic matters

Considering that phase transition occurs more easily between the neighboring regions, we choose the homogeneous opalescent BDDAC/$SOSO_3$ solution (Fig. 2**a, left)** at C_T = 100 mM and x_{BDDAC}= 0.67 as the start to investigate the influence of hydrocarbons on the self-assembly transition. As revealed in Fig. 2**b** and Fig. S3a, the microstructures in this system are vesicles with diameter less than 100 nm. Upon addition of ethylcyclohexane (5 mM), the system is transformed into a stable ASTP in 24 h (Fig. 2**a, right)** at 25 °C. NS-TEM (Fig. 2**c)** and FF-TEM (Fig. S3b**)** results reveal the presence of large fused vesicles with diameter of 500 nm in the upper phase, whereas smaller vesicles about 100 nm are observed in the lower phase (Fig. 2**d,** Fig. S3c**)**. In line with this, the upper phase is shown to be viscous with Newtonian nature, while the lower phase displays water-like fluid behavior (Fig. S4**)**. As ethylcyclohexane is replaced by ethylbenzene, similar ASTP and microstructures are observed (Fig. S5**)**. However, as the cyclic hydrocarbons are replaced by chain-like ones, such as octane, the opalescent homogeneous system becomes clear gradually, and the relative viscosity and the turbidity decreases monotonously (Fig. 3**a** and Fig. 3**b)**. Rheology measurements reveal that the fluids are still Newtonian fluids (Fig. S6**)**. According to DLS analysis (Fig. 3**c)**, the vesicles have transformed into small particles with the average diameter about 9 nm, which are independent on the angle of light scattering (Fig. S7**)**. Moreover, when adding hydrocarbons with different structure into systems at lower concentration C_T = 50 mM (x_{BDDAC}=0.67), these systems follow analogous regulation law to those mentioned above. The formation of larger vesicles (1 μm) with a low curvature is more favored by cyclic hydrocarbons, whereas small particles (9 nm) induced by octane are verified (Fig. S8**)**.

3.2.2. ASTP for addition of organic matters

Next, the influence of hydrocarbons on the C-ASTP with x_{BDDAC}= 0.66 and C_T = 100 mM (Fig. 4**a, left)** is studied. Upon addition of 10 mM ethylcyclohexane or ethylbenzene, the C-ASTP turns to homogeneous phase with birefringence (Fig. 4**a, right)**, which exhibits shear-thinning behavior (Fig. S9a**, b)**. FF-TEM study manifests that Ethylcyclohexane or ethylbenzene has triggered the transition from vesicles to lamellae (Fig. 4**b,** Fig. S10**)**. X-ray diffraction (Fig. S11a**)** reveals three Bragg diffractions peaks correspond to distances of 32.5, 16.0 and 10.8 Å. These data are characteristics for the lamellar phases [37], and the thickness of the lamellae is determined from the (001) diffraction peak to be 32.5 Å. This distance is approximately the sum of the interlaced length of BDDAC and $SOSO_3$ molecules, indicating the lamellae are composed of the bilayers of the mixed BDDAC and $SOSO_3$ molecules (Fig. S11b**)**.

However, the ASTP system becomes water-like as chain-like hydrocarbon, such as octane is added (Fig. 4**c,** Fig. S9c**)**. DLS (Fig. 4**d)** measurement reveals particles in this water-like system are spherical particles with hydrodynamic diameter about 10 nm. Since this size is much larger than the BDDAC/$SOSO_3$ bilayer thickness of 3.25 nm, these spherical particles are probably nanoemulsions of octane stabilized by the BDDAC/$SOSO_3$ monolayers, as demonstrated in Fig. 4**d**.

3.3. Mechanism of hydrocarbon-induced phase transition

The different impact of cyclic and chain-like hydrocarbons on the self-assembly transition in the catanionic surfactant systems can be attributed to their different locations in the hydrophobic surfactant

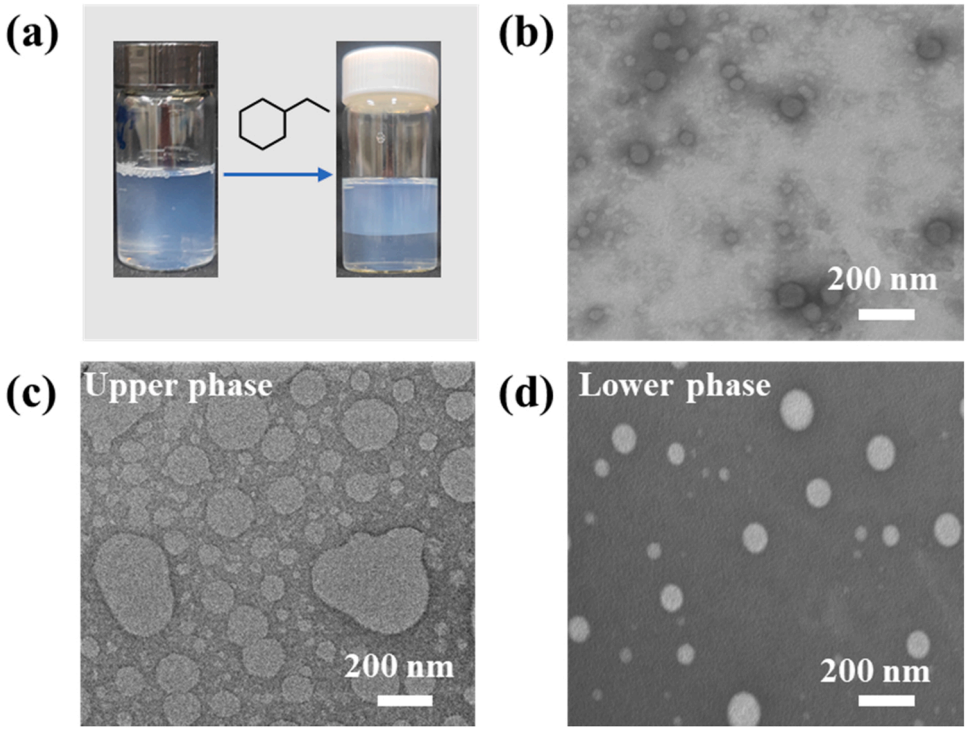

Fig. 2. BDDAC/$SOSO_3$ mixed systems (C_T =100 mM, x_{BDDAC}=0.67, 25 °C). (a) Photographs: left, without additives; right, addition of 5 mM ethylcyclohexane. (b) NS-TEM result without organic matters. NS-TEM images for ASTP after addition of 5 mM ethylcyclohexane: (c) the upper phase; (d) the lower phase.

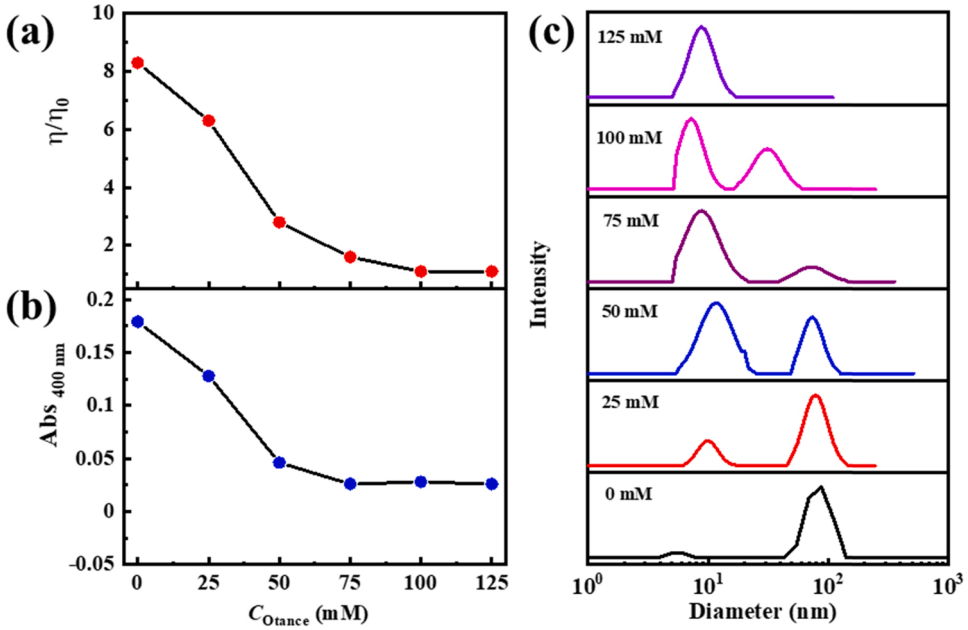

Fig. 3. BDDAC/$SOSO_3$ mixed systems (C_T =100 mM, x_{BDDAC}=0.67, 25 °C) with varied octane concentrations. (a) The variations of relative viscosity, (b) absorbance and (c) DLS.

domains. The well-known theory of the packing parameter p, proposed by Israelachvili et al. has been widely and successfully used to explain the transformations of organized assemblies [38]. According to Israelachvili et al. [38], p is defined as v/a_0l_c, where v is the surfactant tail volume, l_c is the tail length, and a_0 is the mean area per molecule at the aggregate surface. Usually, cyclic hydrophobic molecules are dissolved in the palisade of the surfactant vesicles [36], causing the increase of v. Therefore, an increase in the p can be expected, and formation of larger aggregates with lower curvature is more favored (Scheme 1). However, chain-like substances are generally considered to be solubilized in the interior of hydrophobic region and tend to form an isolated oil droplet between the two half bilayers formed by the tail-to-tail aligned surfactants [35]. As a result, the local curvature of the surfactant bilayers was increased, which finally enclose the oil droplet to form isolated microemulsions (Scheme 2).

To further confirm the above postulation, we conducted the Fluorescence Spectrometry to examine the position of cyclic probe (pyrene) and chain-like molecular (DPH, diphenylhexatriene) in vesicles of

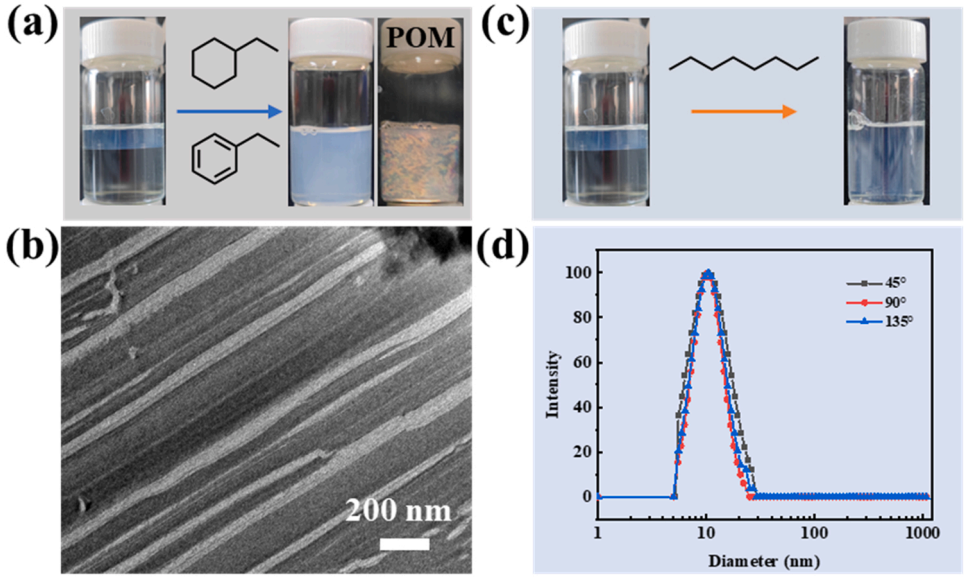

Fig. 4. BDDAC/$SOSO_3$ mixed systems (C_T =100 mM, x_{BDDAC}=0.66, 25 °C) with varied organic additives. (a) Photographs: without additives (left); after addition of 10 mM ethylcyclohexane at visible light (middle) and at the polarizer (right). (b) FF-TEM for addition of 10 mM ethylcyclohexane. (c) Photographs: left, without additives; right, addition of 125 mM octane. (d) DLS results for addition of 125 mM octane at different angles.

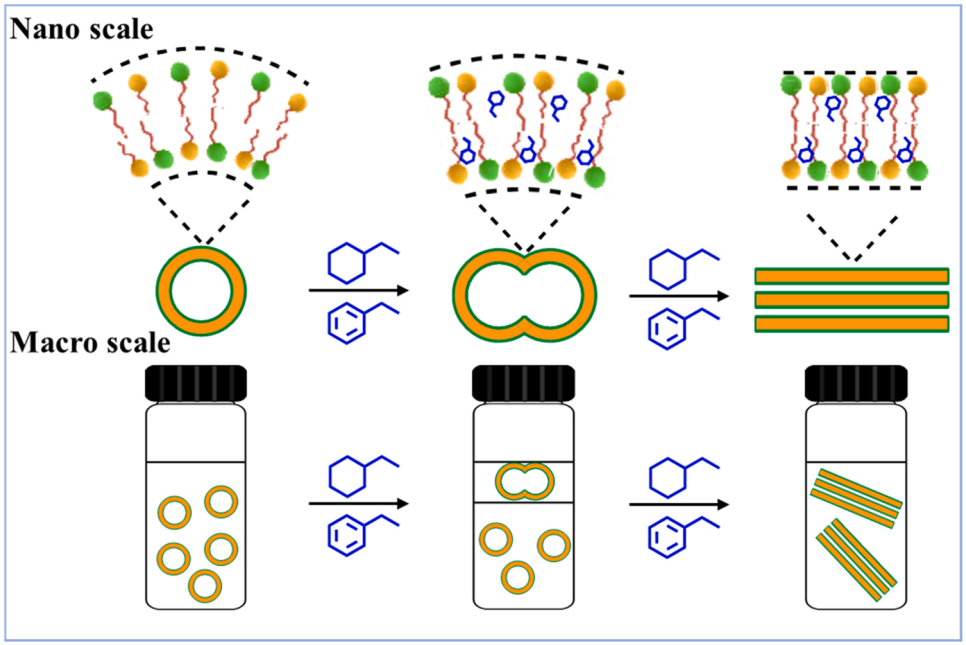

Scheme 1. Schematic illustrations of solubilization locations of ethylcyclohexane and ethylbenzene and phase transition.

BDDAC/$SOSO_3$ system. As shown in Fig. S12, I_1/I_3 ratio of pyrene is 1.12, indicating it is located in palisade of vesicles [39] and the fluorescence anisotropy *r* of DPH is calculated to be 0.09 (Fig. S13), corresponding to the value for inner hydrophobic microenvironment [40]. Analogously, we draw the conclusion that ethylcyclohexane and ethylbenzene are solubilized in palisade , while octane is in interior of hydrophobic region.

4. Conclusion

It can be concluded that the homogeneous phase-ASTP transition in catanionic surfactant systems by addition of organic additives is closely related to the structure of the additive. The rationale is that cyclic hydrophobic molecules are inclined to be dissolved in the palisade of the surfactant bilayers, which increases the volume of the hydrophobic chains thus causing the growth of the self-assembled structures, whereas the chain-like substances are immobilized in the interior of hydrophobic region as an oil droplet. This separates the surfactant bilayers in the middle, and increases the curvature of the outer layer leading to the formation of nanoemulsions. We envision the current work opens a new vista for efficient capture and controllable enrichment of some organic matters.

CRediT authorship contribution statement

Shasha Jiang: Conducted most of the experiments and wrote

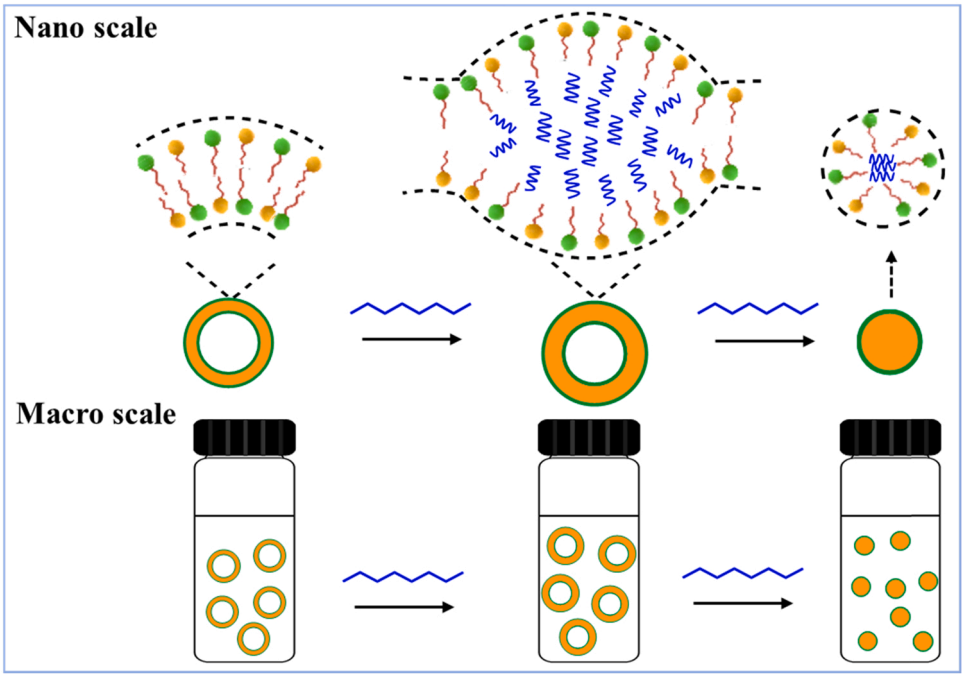

Scheme 2. Schematic illustrations of solubilization location of octane and phase transitions.

original draft. **Xiaoyu Li, Shuitao Gao**, **Cheng Ma, Zhijie Liu, and Jinwan Qi:** Analyzed the data and discussed the results. **Tongyue Wu:** Performed the FF-TEM measurements. **Ting Gu:** Provided DLS results. **Yun Yan:** analyzed the data and revised the paper. **Xinmin Song:** discussed the results and analyzed the data. **Jianbin Huang:** Designed the study, discussed the results and analyzed the data.

Declaration of Competing Interest

The authors declare that they have no known competing financial interests or personal relationships that could have appeared to influence the work reported in this paper.

Acknowledgement

This work is financially supported by the National Natural Science Foundation of China (Grant Nos. 21972003).

Appendix A. Supporting information

Supplementary data associated with this article can be found in the online version at doi:10.1016/j.colsurfa.2022.129231.

References

[1] Q.H. Liang, X.J. Liu, G.M. Zeng, Z.F. Liu, L. Tang, B.B. Shao, Z.T. Zeng, W. Zhang, Y. Liu, M. Cheng, Surfactant-assisted synthesis of photocatalysts: mechanism, synthesis, recent advances and environmental application, Chem. Eng. J. 372 (2019) 429–451.
[2] R. Nandi, S. Laskar, B. Saha, Surfactant-promoted enhancement in bioremediation of hexavalent chromium to trivalent chromium by naturally occurring wall algae, Res. Chem. Intermed. 43 (2017) 1619–1634.
[3] Z.G. Wang, H.T. Zhao, Y. Zhang, A. Natalia, C.A.J. Ong, M.C.C. Teo, J.B.Y. So, H. L. Shao, Surfactant-guided spatial assembly of nano-architectures for molecular profiling of extracellular vesicles, Nat. Commun. 12 (2021) 1–12.
[4] M.D. Kim, S.A. Dergunov, A.G. Richter, J. Durbin, S.N. Shmakov, Y. Jia, S. Kenbeilova, Y. Orazbekuly, A. Kengpeiil, E. Lindner, Facile directed assembly of hollow polymer nanocapsules within spontaneously formed catanionic surfactant vesicles, Langmuir 30 (2014) 7061–7069.
[5] M. Damak, S.R. Mahmoudi, M.N. Hyder, K.K. Varanasi, Enhancing droplet deposition through in-situ precipitation, Nat. Commun. 7 (2016) 1–9.
[6] L. He, S. Xi, L. Ding, B. Li, W. Mu, P. Li, F. Liu, Regulating the entire journey of pesticide application on surfaces of hydrophobic leaves modified by pathogens at different growth stages, ACS Nano 16 (2021) 1318–1331.
[7] X.Z. Hu, H.N. Gong, Z.Y. Li, S. Ruane, H.Y. Liu, E. Pambou, C. Bawn, S. King, K. Ma, P.X. Li, What happens when pesticides are solubilized in nonionic surfactant micelles, J. Colloid Interface Sci. 541 (2019) 175–182.
[8] B. Liu, Y.X. Fan, H.F. Li, W.W. Zhao, S.Q. Luo, H. Wang, B. Guan, Q.L. Li, J.L. Yue, Z.C. Dong, Control the entire journey of pesticide application on superhydrophobic plant surface by dynamic covalent trimeric surfactant coacervation, Adv. Funct. Mater. 31 (2021).
[9] S. Luo, Z. Chen, Z. Dong, Y. Fan, Y. Chen, B. Liu, C. Yu, C. Li, H. Dai, H. Li, Uniform Spread of high-speed drops on superhydrophobic surface by live-oligomeric surfactant jamming, Adv. Mater. 31 (2019).
[10] M.R. Song, D. Hu, X.F. Zheng, L.X. Wang, Z.L. Yu, W.K. An, R.S. Na, C.X. Li, N. Li, Z.H. Lu, Enhancing droplet deposition on wired and curved superhydrophobic leaves, ACS Nano 13 (2019) 7966–7974.
[11] M. Barai, M.K. Mandal, A. Karak, R. Bordes, A. Patra, S. Dalai, A.K. Panda, Interfacial and aggregation behavior of dicarboxylic amino acid-based surfactants in combination with a cationic surfactant, Langmuir 35 (2019) 15306–15314.
[12] Z. Zhai, X. Yan, J. Xu, Z. Song, S. Shang, X. Rao, Phase behavior and aggregation in a catanionic system dominated by an anionic surfactant containing a large rigid group, Chem. Eur. J. 24 (2018) 9033–9040.
[13] H. Hoffmann, W. Ulbricht, Transition of rodlike to globular micelles by the solubilization of additives, J. Colloid Interface Sci. 129 (1989) 388–405.
[14] J.B. Huang, B.Y. Zhu, G.X. Zhao, Z.Y. Zhang, Vesicle formation of a 1: 1 catanionic surfactant mixture in ethanol solution, Langmuir 13 (1997) 5759–5761.
[15] Y. Jiang, F. Li, Y. Luan, W. Cao, X. Ji, L. Zhao, L. Zhang, Z. Li, Formation of drug/surfactant catanionic vesicles and their application in sustained drug release, Int. J. Pharm. 436 (2012) 806–814.
[16] E.W. Kaler, A.K. Murthy, B.E. Rodriguez, J.A.N. Zasadzinski, Spontaneous vesicle formation in aqueous mixtures of single-tailed surfactants, Science 245 (1989) 1371–1374.
[17] Z. Yuan, S. Dong, W. Liu, J. Hao, Transition from vesicle phase to lamellar phase in salt-free catanionic surfactant solution, Langmuir 25 (2009) 8974–8981.
[18] H. Yin, Y. Lin, J. Huang, Microstructures and rheological dynamics of viscoelastic solutions in a catanionic surfactant system, J. Colloid Interface Sci. 338 (2009) 177–183.
[19] L. Zhang, P. Li, X. Liu, L. Du, E. Wang, The effect of template phase on the structures of as-synthesized silica nanoparticles with fragile didodecyldimethylammonium bromide vesicles as templates, Adv. Mater. 19 (2007) 4279–4283.
[20] J.X. Xiao, U. Sivars, F. Tjerneld, Phase behavior and protein partitioning in aqueous two-phase systems of cationic-anionic surfactant mixtures, J. Chromatogr. B 743 (2000) 327–338.
[21] Z. Zhai, X. Yan, J. Xu, Z. Song, S. Shang, X. Rao, Incorporation and recovery of SWNTs through phase behavior and aggregates transition induced by changes in pH in a catanionic surfactants system, Carbon 141 (2019) 618–625.
[22] L.X. Jiang, M.L. Deng, Y.L. Wang, D.H. Liang, Y. Yan, J.B. Huang, Special effect of β-cyclodextrin on the aggregation behavior of mixed cationic/anionic surfactant systems, J. Phys. Chem. B 113 (2009) 7498–7504.

[23] H. Yin, M. Mao, J. Huang, H. Fu, Two-phase region in the DTAB/SL mixed surfactant system, Langmuir 18 (2002) 9198–9203.
[24] X. Xiao, Y. Qiao, Z.R. Xu, T.Y. Wu, Y.X. Wu, Z. Ling, Y. Yan, J.B. Huang, Enzyme-responsive aqueous two-phase systems in a cationic–anionic surfactant mixture, Langmuir 37 (2021) 13125–13131.
[25] M. Yu, Z. Liu, Y. Du, C. Ma, Y. Yan, J. Huang, Endowing a light-inert aqueous surfactant two-phase system with photoresponsiveness by introducing a trojan horse, ACS Appl. Mater. Interfaces 11 (2019) 15103–15110.
[26] Y.C. Liu, A.L.M. Le Ny, J. Schmidt, Y. Talmon, B.F. Chmelka, C.T. Lee Jr., Photo-assisted gene delivery using light-responsive catanionic vesicles, Langmuir (2009) 5713–5724.
[27] G.C. Kalur, B.D. Frounfelker, B.H. Cipriano, A.I. Norman, S.R. Raghavan, Viscosity increase with temperature in cationic surfactant solutions due to the growth of wormlike micelles, Langmuir 21 (2005) 10998–11004.
[28] S. Rajkhowa, S. Mahiuddin, J. Dey, S. Kumar, V. Aswal, R. Biswas, J. Kohlbrecher, K. Ismail, The effect of temperature, composition and alcohols on the microstructures of catanionic mixtures of sodium dodecylsulfate and cetyltrimethylammonium bromide in water, Soft Matter 13 (2017) 3556–3567.
[29] J.C. Hao, H. Hoffmann, Self-assembled structures in excess and salt-free catanionic surfactant solutions, Curr. Opin. Colloid Interface Sci. 9 (2004) 279–293.
[30] L. Jiang, K. Wang, M. Deng, Y. Wang, J. Huang, Bile salt-induced vesicle-to-micelle transition in catanionic surfactant systems: steric and electrostatic interactions, Langmuir 24 (2008) 4600–4606.
[31] Y.Q. Nan, L.S. Hao, Salt-induced phase inversion in aqueous cationic/anionic surfactant two-phase systems, J. Phys. Chem. B 112 (2008) 12326–12337.
[32] J.C. Amante, J.F. Scamehorn, J.H. Harwell, Precipitation of mixtures of anionic and cationic surfactants: II. Effect of surfactant structure, temperature, and pH, J. Colloid Interface Sci. 144 (1991) 243–253.
[33] Y. Lin, X. Han, X. Cheng, J. Huang, D. Liang, C. Yu, pH-regulated molecular self-assemblies in a cationic-anionic surfactant system: from a “1-2″ surfactant pair to a “1-1″ surfactant pair, Langmuir 24 (2008) 13918–13924.
[34] H. Yin, S. Lei, S. Zhu, J. Huang, J. Ye, Micelle-to-vesicle transition induced by organic additives in catanionic surfactant systems, Chem. Eur. J. 12 (2006) 2825–2835.
[35] M. Mao, J. Huang, B. Zhu, J. Ye, The transition from vesicles to micelles induced by octane in aqueous surfactant two-phase systems, J. Phys. Chem. B 106 (2002) 219–225.
[36] M. Mao, J. Huang, B. Zhu, H. Yin, H. Fu, The structural transition of catanionic vesicles induced by toluene, Langmuir 18 (2002) 3380–3382.
[37] M. Wilkins, A. Blaurock, D. Engelman, Bilayer structure in membranes, Nat. New Biol. 230 (1971) 72–76.
[38] J.N. Israelachvili, D.J. Mitchell, B.W. Ninham, Theory of self-assembly of hydrocarbon amphiphiles into micelles and bilayers, J. Chem. Soc., Faraday Trans. 2: Mol. Chem. Phys. 72 (1976) 1525–1568.
[39] P. Lianos, R. Zana, Fluorescence probe studies of the effect of concentration on the state of aggregation of surfactants in aqueous solution, J. Colloid Interface Sci. 84 (1981) 100–107.
[40] E. Feitosa, C.R. Benatti, M.J. Tiera, Effect of sonication on the thermotropic behavior of DODAB vesicles studied by fluorescence probe solubilization, J. Surfactants Deterg. 13 (2010) 273–280.